Design and Synthesis of a Biologically Active Antibody Mimic Based on an Antibody–Antigen Crystal Structure

M. L. Smythe[1] and M. von Itzstein*,[2]

Contribution from the Department of Pharmaceutical Chemistry, Victorian College of Pharmacy, Monash University, 381 Royal Parade, Parkville, Victoria 3052, Australia

Received July 6, 1993®

Abstract: We have used the crystal structure of an N9 sialidase (antigen)–NC41 (antibody) complex to design a low molecular weight compound that mimics the binding function of the macromolecular antibody. The components of recognition between the antibody and the protein antigen have been analyzed from the energy-refined crystal complex. From this analysis, four amino acid residues on the antibody binding surface, which make direct contact with the active-site loop 368–370 of the antigen, have been identified as contributing the majority of the binding energy of the protein. The designed target compound, a constrained cyclic peptide, which mimics the receptor-bound conformation of these amino acids, has been synthesized and found to inhibit N9 sialidase activity, with a K_i of 1×10^{-4} M.

Introduction

Protein antigen–antibody interaction sites are large, burying approximately 1500 Å^2 of surface area upon complexation.[4] Their combining sites comprise approximately 15–20 amino acid residues for the three-dimensional structures determined to date.[4-8] Clearly, if all of these residues on the protein binding sites are making equal contributions toward the binding energy between the two proteins, then the task of mimicking the protein binding regions with low molecular weight compounds would be difficult. However, results from competitive experiments of monoclonal and polyclonal antibodies suggest that four, or even less, residues are sufficient to define an antigenic epitope.[9] Similarly, synthetic peptides derived from amino acid sequences of complementarity-determining regions (CDR's) may have analogous binding properties to those of the intact antibody.[10] Further, Novotny *et al.* have concluded, from theoretical calculations, that "protein antigenicity involves active, attractive contributions mediated by a few energetic amino acids and a passive surface complementarity contributed by the surrounding surface area".[11]

These data suggest that it may be possible to mimic protein sites, with low molecular weight compounds. The initial study requires the identification of the key ("energetic") amino acid residues on the protein binding sites, followed by the design and synthesis of compounds that mimic the receptor-bound conformation of these key amino acid residues. One would imagine that the protein mimetic would have a lower affinity than the parent protein simply due to the difference in bound surface area (and hence a potential loss of enthalpic and hydrophobic stabilization) of the mimetic versus that of the parent protein.

Our recent interest in sialidases,[12] in particular the design and synthesis of novel influenza sialidase inhibitors as potential anti-influenza drugs,[13] has also led us to the study of an N9 sialidase–NC41 antibody complex. The crystal structure of the complex between influenza viral enzyme sialidase (subtype N9, isolated from an avian source) and the Fab of a monoclonal antibody NC41 (Figure 1) has been determined by Colman *et al.*[7,8] The interface between N9 and NC41 shows a high degree of steric complementarity. There is a groove between antibody NC41 V_L and V_H domains that accommodates a large ridge on the antigenic surface of N9 sialidase. Adjacent to this, CDR H3 of antibody NC41 forms a ridge which matches a pocket on N9 sialidase which is formed by residues 368–370 and 400–403. The enzymic activity of N9 sialidase is inhibited by the binding of antibody NC41,[7,14] and a binding affinity for the complex of 1.2×10^{-7} M has been determined.[15]

Some indication of the mechanism of inhibition by antibody NC41 can be obtained from the crystal structure of the sialidase–sialic acid complex.[16] On the basis of this structure, it has been

* Abstract published in *Advance ACS Abstracts*, February 15, 1994.

(1) Currently a postdoctoral fellow at the Centre for Molecular Design, Washington University, St. Louis, MO, 63130-4899.

(2) To whom correspondence should be addressed.

(3) Abbreviations: Boc, N^{α}-*tert*-butyloxycarbonyl; BOP, benzotriazol-1-yloxytris(dimethylamino)phosphonium hexafluorophosphate; CDR, complementarity-determining region; cHx, cyclohexyl; DCC, 1,3-dicyclohexylcarbodiimide; DCM, dichloromethane; DIPEA, diisopropylethylamine; DMF, *N*,*N*-dimethylformamide; d_6-DMSO, dimethyl sulfoxide-d_6; DQFCOSY, double quantum filtered correlated spectroscopy; Fab, antigen binding fragment; Fmoc, 9-fluorenylmethoxycarbonyl; fs, femtosecond; HOBt, 1-hydroxybenzotriazole; HPLC, high-performance liquid chromatography; Hz, Hertz; kcal, kilocalorie; Id, nonpolar atoms; K_i, dissociation constant fo inhibitor; pMBHA, *p*-methylbenzhydrylamine; MES, (2-*N*-morpholino)ethanesulfonic acid; MHz, megahertz; min, minute(s); mL, milliliter(s); mmol, millimole(s), mp, melting point; NMM, *N*-methylmorpholine; NMR, nuclear magnetic resonance; NOE, nuclear Overhauser effect; ps, picosecond; RMS, root mean square; ROESY, rotating frame Overhauser enhancement spectroscopy; *t*Bu, *tert*-butyl; TFA, trifluoroacetic acid; TLC, thin-layer chromatography; TOCSY, total correlated spectroscopy; V_H, variable heavy chain; V_L, variable light domain.

(4) Davies, D. R.; Sheriff, S.; Padlan, E. A. *J. Biol. Chem.* **1988**, *263*, 10541–10544.

(5) Amit, A. G.; Mariuzza, R. A.; Phillips, S. E. V.; Poljak, R. J. *Science* **1986**, *233*, 747–753.

(6) Sheriff, S.; Silverton, E. W.; Padlan, E. A.; Cohen, G. H.; Smith-Gill, S. J.; Finzel, B. C.; Davies, D. R. *Proc. Natl. Acad. Sci. U.S.A.* **1987**, *84*, 8075–8079.

(7) Colman, P. M.; Laver, W. G.; Varghese, J. N.; Baker, A. T.; Tulloch, P. A.; Air, G. M.; Webster, R. G. *Nature* **1987**, *326*, 358–363.

(8) Tulip, W. R.; Varghese, J. N.; Laver, W. G.; Webster, R. G.; Colman, P. M. *J. Mol. Biol.* **1992**, *227*, 122–148.

(9) (a) Kabat, E. A. *Ann. N. Y. Acad. Sci.* **1970**, *169*, 43–54. (b) Schechter, I. *Ann. N. Y. Acad. Sci.* **1971**, *190*, 394–419. (c) Hodges, R. S.; Heaton, R. J.; Parker, J. M. R.; Molday, L.; Molday, R. S. *J. Biol. Chem.* **1988**, *263*, 11768–11775.

(10) (a) Taub, R.; Gould, R. J.; Garsky, V. M.; Ciccarone, T. M.; Hoxie, J.; Friedman, P. A.; Shattil, S. J. *J. Biol. Chem.* **1989**, *264*, 259–265. (b) Williams, W. V.; Guy, H.; Rubin, D.; Robey, F.; Meyers, F.; Kieber-Emmons, T.; Weiner, D.; Greene, M. *Proc. Natl. Acad. Sci. U.S.A.* **1988**, *85*, 6488–6492. (c) Williams, W. V.; Moss, D. A.; Kieber-Emmons, T.; Cohen, J. A.; Myers, J. N.; Weiner, D. B.; Greene, M. *Proc. Natl. Acad. Sci. U.S.A.* **1989**, *86*, 5537–5541. (d) Saragovi, H. U.; Fitzpatrick, D.; Raktabutr, A.; Hiroshi, N.; Kakn, M.; Greene, M. I. *Science* **1991**, *253*, 792–795.

(11) Novotny, J.; Bruccoleri, R. E.; Saul, F. A. *Biochemistry* **1989**, *28*, 4735–4746.

(12) (a) Chong, A. K. J.; Pegg, M. S.; von Itzstein, M. *Biochim. Biophys. Acta* **1991**, *1077*, 65–71. (b) Chong, A. K. J.; Pegg, M. S.; von Itzstein, M. *Biochem. Int.* **1991**, *24*, 165–171. (c) Chong, A. K. J.; Pegg, M. S.; Taylor, N. R.; von Itzstein, M. *Eur. J. Biochem.* **1992**, *207*, 65–71.

(13) (a) von Itzstein, M.; Wu, W.-Y.; Van Phan, T.; Danylec, J.; Jin, B. *Chem. Abstr.* **1991**, *117*, 49151y. (b) Holzer, C. T.; von Itzstein, M.; Jin, B.; Pegg, M. S.; Stewart, W. P.; Wu, W.-Y. *Glyconconjugate J.* **1993**, *10*, 40–45. (c) von Itzstein, M., *et al. Nature* **1993**, *363*, 418–423.

0002-7863/94/1516-2725$04.50/0

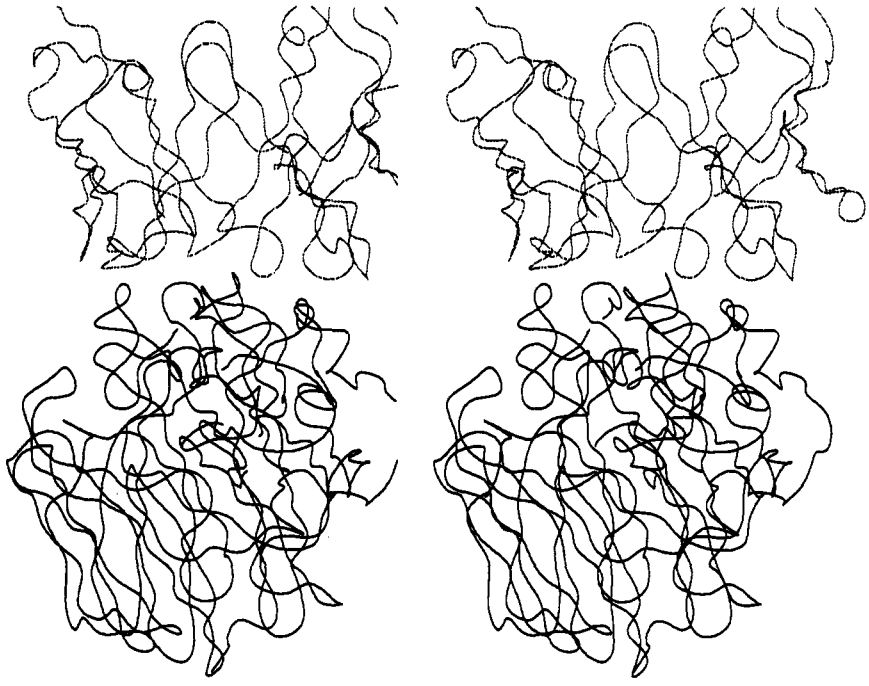

Figure 1. Stereoscopic view of the complex between antigen N9 sialidase and antibody NC41. The upper protein is the variable domains of antibody NC41, and the lower protein is the antigen N9 sialidase.

recently proposed that the antibody NC41 inhibits the enzyme N9 sialidase by binding to the active-site loop 368–370 and so sterically interfering with the approach of the substrate. Analysis of this complex suggests that the approach of the substrate into the active site places the sialoside aglycon moiety near sialidase residues 368–370. Upon binding, the sialoside is known to be conformationally distorted[12] away from a $^2C_5$ conformation, leaving the aglycon positioned directly above the site, well removed from residues 368–370.

We report here the design, synthesis, and biological evaluation of an antibody NC41 mimic based on an analysis of the crystal structure of the N9 sialidase–NC41 antibody complex. It is proposed that this antibody mimic binds to the active-site loop 368–370 of the antigen and inhibits enzyme activity by sterically interfering with the approach of the substrate.

Experimental Section

Analysis of N9 Sialidase–Antibody NC41 Complex. Atomic coordinates of the N9 sialidase–NC41 antibody complex (2.5 Å, *R*-factor 0.191) were kindly provided by Dr. P. Colman and colleagues (Division of Biomolecular Engineering, CSIRO). The complex was energy-refined, using a combination of steepest descents and conjugate gradient minimizations, with the AMBER (v 3.0)[17] software package, to a gradient of less than 0.01 kcal/(mol/Å). The AMBER united-atom force field, a nonbonded cutoff of 8.0 Å, and a distance-dependent dielectric function were employed.

In order to gauge how electrostatically complementary the two protein binding surfaces are in relation to their interactions with solvent, the protein binding sites were solvated with an 8.0-Å layer of equilibrated water molecules using the in-house program CONTACT.[18] These conformations were then minimized to a gradient of less than 0.01 kcal/(mol/Å) (using the AMBER united-atom force field) with the protein held fixed. Molecular dynamic simulations (employing a constant dielectric of 1.0, an 8.0-Å cutoff, and a 1-fs time step) of the solvated protein binding sites were accomplished with the DISCOVER (v 2.6)[19] implementation of the AMBER united-atom force field. The water molecules were subjected to a total of 15 ps of molecular dynamics at 300 K. The protein was held fixed during these simulations.[20] At 1-ps intervals the instantaneous conformation was minimized to a gradient of less than 0.01 kcal/(mol/Å). The lowest energy conformation found was used in the analysis procedure.

The analysis procedure comprised an enthalpic and a nonbonded geometrical calculation of the antibody–antigen interaction in order to determine the key ("energetic") components of the interaction. The process comprised the use of the program CONTACT and the analysis module (anal) of AMBER. The energy-refined complex and the solvated protein conformations were subjected to the analysis process. For the geometrical nonbonded analysis (using program CONTACT), atoms were considered to form intermolecular contacts if their separation distance was within the sum of their van der Waals radii plus 1.0 Å. The program categorized such contacts into charged, polar and nonpolar classes. When any dipole contacts (polar) were considered, the angular component of the contact was calculated.[18] Charged atoms were defined as the charged atoms of residues Glu, Asp, Lys, Arg, and N^{δ} of His. Polar atoms were defined as noncharged heteroatoms and carbons that are bonded to heteroatoms. Nonpolar atoms (Id) were defined as carbon atoms that are solely bonded to carbon atoms. The analysis module of AMBER was used to calculate the enthalpy of interaction of each antibody residue with N9 sialidase. A distance-dependent dielectric and an 8.0-Å cutoff were used for this calculation. Such information allowed us to identify a key loop on the antibody surface that appears to contribute a significant amount of the interaction energy (Table 1).

Design

Organic Scaffold Design. Having identified a key loop (CDR H3) on the antibody surface, the next stage was to design a compound whose conformation was restricted to the receptor-bound conformation of this key loop. The first stage of the design process involved the design of compounds that mimicked the receptor framework (defined in Figure 2) of the key antibody

(14) Colman, P. M.; Air, G. M.; Webster, R. G.; Varghese, J. N.; Baker, A. T.; Lentz, M. R.; Tulloch, P. A.; Laver, W. G. *Immunology Today* **1987**, *8*, 323–326.

(15) Gruen, L. C.; McInerney, T. L.; Jackson, D. C.; Webster, R. G. *J. Protein Chem.* **1993**, *12*, 255–259.

(16) Varghese, J. N.; McKimm-Breschkin, J. L.; Caldwell, J. B.; Kortt, A. A.; Colman, P. M. *Proteins* **1992**, *14*, 327–332.

(17) Weiner, S. J.; Kollman, P. A.; Case, D. A.; Singh, U. C.; Ghio, C.; Alagona, G.; Progeta, S., Jr.; Weiner, P. *J. Am. Chem. Soc.* **1984**, *106*, 765–784.

(18) Smythe, M. L. Design and Synthesis of Protein Mimics. Ph.D. Thesis, Victorian College of Pharmacy, University of Melbourne, Australia, 1992.

(19) Biosym Technologies Inc., 9685 Scranton Rd., San Diego, CA 92121-2777.

(20) It is important to recognize that such an approach used for analysis of protein solvation is based on the assumption that the two proteins would interact in a fashion similar to a "lock and key". In this way the solvated protein conformation would be identical to that found in the complex.

Table 1. Analysis of the Protein Complex[a]

	buried charge–charge	charge–polar	polar–polar	Hbond	charge–Id	polar–Id	Id–Id	enthalpy (kcal/mol)
NC41-N9	1	18	84	26	19	222	49	–63.6[b]
L49-L56	0	0	24	4	0	75	14	–10.5
L91-L96	0	3	10	4	4	21	7	–10.1
H30-H32	0	0	23	3	0	24	8	–7.3
H50-H54	0	0	3	2	0	66	13	–2.8
H96-H99	1	11	23	10	14	61	8	–32.9

[a] A summary of the number of contacts of each loop of the antibody with the antigen. The entire antibody is represented as NC41-N9. Id represent nonpolar atoms. [b] This enthalpy represents the sum of the interaction energy of the individual loops listed in the above table. The total protein–protein interaction energy was calculated as –73.4 kcal/mol.

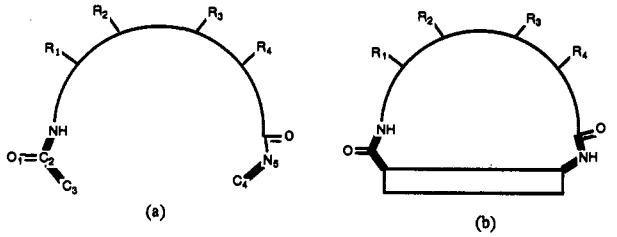

Figure 2. (a) Receptor loop framework (thick lines) describing the initiation and termination of the loops of interest. The receptor framework is defined as the distance between C_2 and N_5 and dihedral angles between the two vectors C2–C3 and C4–N5. For the key antibody loop (CDR H3) the receptor framework was calculated as 5.5 Å (C2–N5 distance), –56.8° (C2–C3–C4–N5 dihedral angle), and –55.6° (O1–C2–C3–C4 dihedral angle). (b) Organic scaffolds are designed that accommodate both the distance spanning the loop (C3–C4) and the C2–C3 and C4–N5 vectors.

loop. Thus, atomic distances and dihedral angles that define the geometry of the receptor framework of the key antibody loop (CDR H3) were calculated. Organic "scaffolds", considered in the design process, were built using the build module in MACROMODEL (v 1.5).[21] The compounds were energy-refined using the implementation of the MM2 force field in MACROMODEL. The dihedral angles and distances defining the receptor framework geometry of the protein loop were then applied as constraints to the molecules. The constrained conformation was minimized to a gradient of less than 0.02 kcal/(mol/Å). A force constant of 5 kcal/(mol/Å) was used for this calculation. These calculations were performed using a distance-dependent dielectric and a cutoff of 13 Å for both van der Waals and electrostatic interactions. The resulting conformation (E_{con}) was then superimposed onto the desired receptor framework, and the root mean square of superimposition over the five receptor template atoms was calculated. If the root mean square was suitable (less than 0.5 Å), then the molecule was subjected to a conformational search. This was necessary in order to gauge the energy accessibility of the receptor framework conformation of the organic scaffold.

Conformational searching was achieved using the multiconformer module of MACROMODEL. The torsion angles defining the rotation about the amine and the carboxyl functional groups were rotated in 10-deg increments. Conformations that had no nonbonded interactions under 1.5 Å were collected. These conformations were energy-minimized to a gradient of 0.02 kcal/(mol/Å) using MM2. If the resulting conformations were unique and were within 5 kcal/mol above the lowest energy conformation found, they were subsequently stored. If the designed organic scaffolds had a suitable root mean square and the E_{con} conformation was within 5 kcal/mol above the lowest energy conformation found (E_{min}), these structures were submitted to the second phase of the design process (template force).

Template Force. After constraining the entering and leaving angles of the loop, by an organic scaffold, the second phase of the design process was to determine how well this scaffold "holds" the peptide in the desired receptor-bound conformation. The constrained cyclic peptides were built using INSIGHT II (v 2.1.0).[19] The receptor conformation of the antibody loop was extracted from the antibody coordinates. The side-chain atoms of the constrained cyclic peptide were template-forced onto the receptor loop side-chain atoms. This involved a constrained minimization of the cyclic peptide to a gradient of less than 0.01 kcal/(mol/Å) using a combination of steepest descents and conjugate gradient minimizations. This was done with the DISCOVER (v 2.6) program. The DISCOVER force field (CVFF, without Morse potentials or crossterms) was used with a template-forcing constant of 20 kcal/(mol/Å). The energy of this conformation (E_{force}) and the root mean square superimposition of the side-chain atoms with the desired receptor conformation were then calculated.

High-Temperature Molecular Dynamics Conformational Search. In order to gauge the energy accessibility of the receptor-bound conformation, and hence how well the scaffold holds the peptide in the desired receptor-bound conformation, a conformational search was conducted. The template-forced conformation (E_{force}) was minimized (with no constraints in place) to a gradient of 0.01 kcal/(mol/Å) prior to molecular dynamics. This conformation was equilibrated for 20 ps at 800 K and molecular dynamics resumed for another 100 ps at that temperature. A 1-fs time step was used, and the amide bonds were constrained to a *trans*[22] geometry with a force constant of 5 kcal/(mol/Å). At every 1 ps a structure was collected and minimized to a gradient of less than 0.01 kcal/(mol/Å), using a combination of steepest descents and conjugate gradient minimizations. The difference between the template-forced conformation (E_{force}) and the lowest energy conformation found (E_{min}) was used to gauge the effectiveness of the scaffold.

Synthesis

Materials and Methods. *p*-Methylbenzhydrylamine (pMBHA) resin (0.82 mmol/g) was used as a polymer support. N^{α}-*tert*-butoxycarbonyl- (Boc) and N^{α}-fluorenylmethyloxycarbonyl- (Fmoc) protected amino acids were purchased from Auspep Pty Ltd., Australia. The Fmoc–Asp(OcHx)–OH and Fmoc–Glu(OcHx)–OH amino acids were prepared from their Boc derivatives by trifluoracetic acid deprotection and Fmoc protection.[23] Fmoc–Asp(OH)O*t*Bu was purchased from Bachem. All reagents and solvents were AR grade and were used without further purification. Mass spectra (FAB) were recorded on a Jeol JMS-Dx 300 double-focusing instrument, with a Jeol-FABMS source and argon as incident particle, in a thioglycerol/glycerol matrix. All infrared spectra were recorded using a Hitachi 370–30 spectrophotometer. Melting points were determined on a Reichter micro-melting point apparatus and are uncorrected. All proton NMR spectra

(21) Mohamadi, F.; Richards, N. G.; Guida, W. C.; Liskamp, R.; Lipton, M.; Caulfield, C.; Chang, G.; Hendericksen, T.; Still, W. C. *J. Comput. Chem.* **1990**, *11*, 440–467.

(22) This was used to eliminate *cis–trans* interconversion, which has been shown to be a useful strategy in high-temperature molecular dynamics. *Discover User Guide Part I*; Biosym Technologies: San Diego, CA, 1992; Version 2.6.

(23) Milton, R. C.; Becker, E.; Milton, S. C. F.; Baxter, J. E. J.; Elsworth, J. E. J. *Int. J. Pept. Protein Res.* **1987**, *30*, 431–432.

were recorded at 300.133 MHz on a Brüker AM-300 or AMX-300 spectrometer. Chemical shifts are quoted as δ values (ppm) relative to an internal tetramethylsilane standard. Coupling constants (J) are given in Hertz, with observed single multiplicity designated as s (singlet), d (doublet), t (triplet), q (quartet), m (multiplet) and b (broad).

Preparation of the Scaffold (3-(((9-Fluorenylmethoxycarbonyl)amino)methyl)benzoic acid) (3) (Fmoc-Amb-OH)

3-(Phthalimidomethyl)benzoic Acid (1).[24] A cold (0 °C) solution of benzoic acid (1.2 g, 10 mmol) and *N*-(hydroxymethyl)-phthalimide[25] (1.77 g, 10 mmol) in concentrated sulfuric acid was reacted overnight at 0 °C. The reaction was quenched by addition of the mixture to ice/water, and the title compound (**1**) (2.3 g, 80%) was collected by filtration and dried *in vacuo*: mp 227–230 °C, lit. mp[24] 228.5–230.5 °C; ^{1}H NMR (d_6-DMSO) 4.83 (s, CH_2), 7.4–8.1 (m, aromatics); IR (KBr) 2964, 1768, 1710, 1452, 1418, 1324, 704 cm^{-1}; MS (FAB) 282 (m/z + 1), 264, 185, 110.

3-(Aminomethyl)benzoic Acid (2).[24] To a stirred solution of 3-(phthalimidomethyl)benzoic acid (**1**) (0.44 g, 1.6 mmol) in a mixture of 2-propanol (14 mL) and water (2.4 mL) was added $NaBH_4$ (0.3 g, 8 mmol). After the reaction was stirred for 24 h, TLC indicated the complete disappearance of starting material. Glacial acetic acid (1.6 mL) was carefully added, and when the exothermic reaction subsided, the flask was stoppered and heated at 80 °C for 2 h.

The crude reaction mixture was loaded onto a Dowex 50 (H^+) column washed with water (750 mL) and then eluted with 1 M NH_4OH (500 mL). Ninhydrin-active fractions were collected and pooled for freeze drying, affording 3-(aminomethyl)benzoic acid (**2**) (0.17 g, 45%), mp 244–246 °C, lit. mp[24] 246–249 °C.

3-(((9-Fluorenylmethoxycarbonyl)amino)methyl)benzoic Acid (3) (Fmoc-Amb-OH). 3-(Aminomethyl)benzoic acid (**2**) (0.75 g, 5 mmol) was dissolved in water (5 mL), and the pH of this solution was adjusted to 8 by the addition of triethylamine. To this solution at 0 °C was added (9-fluorenylmethyl)succinimidyl carbonate (1.5 g, 4.5 mmol) in acetonitrile (5 mL). The pH of the solution was monitored and kept at ≈8, by addition of triethylamine. With the pH constant, the reaction mixture was allowed to stir at room temperature for 3 h. The reaction mixture was filtered, and the solvent was removed under reduced pressure. The isolated residue was added to a vigorously stirred 1 M HCl solution. The resulting precipitate was collected by filtration, dissolved in ethyl acetate, and washed with several portions of 1 M HCl. After removal of solvent under reduced pressure, the product was purified by recrystallization from ethyl acetate/hexane to give 3-(((9-fluorenylmethoxycarbonyl)amino)methyl)-benzoic acid (**3**) (1.27 g, 68%); mp 200–201 °C; ^{1}H NMR (MeOH-d_4) 4.12 (t, 1H, J = 6.8 Hz), 4.24 (s, CH_2–N), 4.28 (d, 2H, J = 6.8 Hz), 7.3 (m, 8H), 7.56 (d, 2H, J = 7.3 Hz), 7.68 (d, 2H, J = 7.44 Hz), 7.82 (dt, H6, J = 7.5, 1.5 Hz), 7.89 (bs, H2); MS (FAB) 374 (m/z + 1), 192, 178; HRMS (FAB) Obsd 373.1292 ($C_{23}H_{19}N_1O_4$), Reqd 373.1315.

Peptide Synthesis. All peptides were prepared manually using a solid-phase peptide synthesis vessel, equipped with a Griffin shaker system.

Synthesis of Antibody Mimic (5). pMBHA resin (5 g, 0.82 mmol substitution) was neutralized by two successive 10-min washes with 10% DIPEA/DCM. The first amino acid (Fmoc-Asp(OH)-O*t*Bu) was attached to the resin, as its preformed HOBt ester, to give a resin substitution of 0.5 mmol/g.[26] The substitution on the resin was calculated using a spectrophotometric technique.[27] The remaining amino groups were blocked by acetylation using acetic anhydride (1.5 mL) in DCM-containing pyridine (3.5 mL) for 20 min at room temperature. On a 2-g (1 mmol) scale of resin, the remaining amino acid residues (including the constraint) were added to the growing peptide chain by the sequential stepwise addition of a 2 molar excess of Fmoc-Asp(OcHx)-OH, Fmoc-Glu(OcHx)-OH, Fmoc-Amb-OH followed by Boc-Phe-OH using standard solid-phase synthetic methodologies.[28] Each coupling reaction was carried out using a twofold excess of BOP and HOBt and a threefold excess of NMM. Following coupling of the last amino acid, the *t*Bu and Boc protecting groups were removed by treatment of the peptide resin with 60% TFA/DCM for 45 min. The peptide resin was washed with DCM (4 × 1 min), DMF (2 × 1 min), 10% DIPEA/DMF (2 × 2 min), and DMF (3 × 1 min). Cyclization was achieved by suspension of the resin in DMF (15 mL) and the addition of a threefold excess of BOP/HOBt and 1.6 equiv of DIPEA. The cyclization reaction was monitored by the quantitative ninhydrin assay and was found to be complete after 5 days. A fresh excess of coupling reagents was added every 24 h. The peptide was cleaved from the resin using anhydrous HF in the presence of anisole as the scavenger. The peptide was extracted with 0.1% TFA–30% acetonitrile/water and subsequently water and then lyophilized to yield 360 mg of crude product. The crude product was purified by reverse-phase HPLC on a μ-Bondpack C18 (10 μm, 125 Å) (25 mm × 100 mm) column, eluted with a linear acetonitrile gradient (20–40%), over 50 min with a flow rate of 4.8 mL/min, with a constant concentration of trifluoroacetic acid (0.1% v/v). The linear gradient was generated with a Waters 600 E system controller. The separation was monitored at 230 nm with a Waters 484 tunable absorbance detector and integration achieved with the Baseline software package. Two major products were isolated and were characterized as the target constrained cyclic peptide (**5**) in 5% yield and an imide byproduct (**6**). The amino acid analysis of the constrained cyclic peptide agreed with expectations. Fraction 1: MS 639 (m/z + 1), corresponding to the target cyclic constrained peptide (**5**) ($C_{30}H_{34}N_6O_{10}$). ^{1}H NMR data (d_6-DMSO) are summarized in Table 3. Fraction 2: MS 621 (m/z + 1), corresponding to the imide byproduct (**6**) ($C_{30}H_{32}N_6O_9$); ^{1}H NMR (d_6-DMSO) 2.0 (m, Glu $C_\beta H_2$), 2.40 (t, Glu, $C_\gamma H_2$), 2.54 (m, Asp $C_\beta H''$), 2.54 (m, Asn $C_\beta H''$), 3.06 (m, Phe $C_\beta H''$), 3.06 (m, Asp $C_\beta H'$), 3.06 (m, Asn $C_\beta H'$), 3.35 (dd, Phe $C_\beta H'$), 4.05 (m, Amb–CH_2'), 4.30 (m, Amb–CH_2'), 4.37 (m, Asp $C_\alpha H$), 4.59 (m, Glu $C_\alpha H$), 4.75 (m, Amb–CH_2''), 4.75 (m, Phe $C_\alpha H$), 5.24 (m, Asn $C_\alpha H$), 7.18–7.55 (m, aromatic), 7.55 (d, Phe NH), 7.90 (d, Glu NH), 8.53 (m, Amb NH), 9.42 (m, Asp NH).

Synthesis of Linear Peptide Ac-Glu-Asp-Asn-Phe-NH_2 (7). pMBHA resin (2 g, 0.46 mmol substitution) was neutralized by two successive 10-min washes with 10% DIPEA/DCM. The first amino (Boc-Phe-OH, 0.49 g, 1.84 mmol) was attached to the resin as its symmetrical anhydride. The degree of coupling on the resin was determined by quantitative ninhydrin assay, and the resin was blocked by acetylation with acetic anhydride. On a 2-g (0.92 mmol) scale of resin, the remaining amino acid residues were added using standard solid-phase methodologies.[28] Boc-Asn-OH was coupled as its HOBt ester, and the remaining amino acids (Boc-Asp(OBzl)-OH and Boc-Glu(OBzl)-OH) were coupled as symmetrical anhydrides. After addition of the last amino acid, it was deprotected by treatment with 40% TFA/DCM, neutralized with a 10% DIPEA/DCM wash, and acety-

(24) Oda, R.; Teramura, K.; Tanimoto, S.; Motaki, N.; Suda, H.; Matsuda, K. *Bull. Inst. Chem. Res., Kyoto Univ.* **1955**, *33*, 117–122; *Chem. Abstr.* **1957**, *51*, 11355d.

(25) Buc, S. R. *J. Am. Chem. Soc.* **1947**, *69*, 254–256.

(26) Effects of resin substitution on peptide yields: Plaue, S. *Int. J. Pept. Protein Res.* **1990**, *35*, 510–517.

(27) Meienhofer, J.; Waki, M.; Hiemer, E. P.; Lambros, T. J.; Makofske, R. C.; Chang, C.-D. *Int. J. Pept. Protein Res.* **1979**, *23*, 35–42.

(28) (a) Bodanszky, M. *Principles of Peptide Synthesis*; Springer-Verlag: Heidelberg, Germany, 1984. (b) Barany, G.; Merrifield, R. B. In *The Peptides*; Gross, E., Meienhofer, J., Eds.; Academic Press: New York, 1980; Vol. 2. (c) Stewart, J. M.; Young, J. D. *Solid State Phase Peptide Synthesis*, 2nd ed.; Pierce Chemical Company: Rockford, IL, 1984. (d) Barany, G.; Kneib-Cordonier, N.; Mullen, D. G. *Int. J. Pept. Protein Res.* **1987**, *30*, 705–739.

lated with acetic anhydride. The peptide was cleaved from the resin using anhydrous HF in the presence of the scavenger, anisole. The peptide was extracted with 0.1% TFA–30% acetonitrile/water and subsequently water and then lyophilized to yield 260 mg of crude product. The crude product was purified by reverse-phase HPLC, using a linear acetonitrile gradient (10–50%) over 60 min with a flow rate of 4.8 mL/min to give **7** (19%). Amino acid analyses were consistent with the desired product: MS 565 (m/z + 1) $C_{24}H_{32}O_{10}N_6$; ^{1}H NMR (d_6-DMSO) δ 1.71 (m, Glu $C_\beta H_2$), 1.85 (s, CH_3), 2.24 (t, Glu $C_\gamma H_2$), 2.33 (dd, Asn $C_\beta H'$), 2.49 (m, Asn $C_\beta H''$), 2.49 (m, Asp $C_\beta H'$), 2.62 (dd, Asp $C_\beta H''$), 2.79 (dd, Phe $C_\beta H''$), 3.08 (dd, Phe C_β'), 4.20 (m, Glu $C_\alpha H$), 4.28 (m, Phe $C_\alpha H$), 4.41 (m, Asn $C_\alpha H$), 4.48 (m, Asp $C_\alpha H$), 6.92 (s, amide NH), 7.21 (s, amide NH), 7.91 (d, Phe NH), 7.97 (d, Asn NH), 8.05 (d, Glu NH), 8.22 (d, Asp NH).

Characterization and Structure Determination of Antibody Mimic. A 16 mM sample of the antibody mimic (**5**) was prepared by dissolving 7 mg of compound **5** in 0.7 mL of d_6-DMSO. ^{1}H NMR spectra were recorded with a Brüker AMX-300 spectrometer and processed on a Silicon Graphics 4D/25 workstation using the software package FELIX.[29] These experiments included a TOCSY spectrum with a mixing time of 80 ms, a DQFCOSY, and three ROESY spectra with mixing times of 250, 150, and 80 ms. Apart from the temperature studies, all experiments were recorded at 30 °C. All spectra were run with a spectral width of 3030.3 Hz. 1D spectra were recorded with 16K data points, multiplied by a 60° phase-shifted sine bell squared function, and zero-filled to 32K prior to Fourier transformation. The DQFCOSY of the antibody mimic (**5**) was acquired with 4096 data points for each of the 800 t_1 values and 64 transients. Prior to Fourier transformation the time domain was multiplied in both dimensions by a 90° phase-shifted sine bell. The length of the window function in all 2D experiments was adjusted to reach zero at the last experimental point in the t_1 and t_2 directions. $^3J_{NH-CH}$ coupling constants were measured for the antibody mimic (**5**) by selecting appropriate traces from the DQFCOSY spectrum and subjecting each slice to an inverse Fourier transformation, zero-filling to 8K, applying a 60° phase-shifted sine bell, and finally a Fourier transformation. The $^3J_{NH-CH}$ were then measured directly from the modified traces (Table 3). The TOCSY and ROESY experiments of the antibody mimic (**5**) were acquired with 1024 data points for each of the 400 t_1 values and 32 transients. The temperature dependence of the amide protons were measured at 25, 30, 37, and 42 °C.

Solution Conformation. A total of 15 approximate interproton distance constraints, including 13 interresidue constraints were derived from the ROESY spectra.[18] These distances were classified as 2.7, 3.5, and 5.0 Å for strong, medium, and weak crosspeaks.[30] Pseudoatoms (average atoms) were used for the C_β protons of Asp, Asn, and Phe, and the C_γ protons of Glu, and the CH_2 of Amb. With the constraints in place the conformation was minimized, using steepest descents and conjugate gradients, down to a gradient of less than 0.01 kcal/(mol/Å) using the DISCOVER program. A distance-dependent dielectric, a non-bonded cutoff of 12 Å, and a harmonic force constant of 100 kcal/(mol/Å) were used for these calculations. This conformation was equilibrated for 20 ps of restrained molecular dynamics at 800 K and resumed for 100 ps with a 1-fs time step at this temperature. At every 1 ps the instantaneous structure was minimized to a gradient of less than 0.01 kcal/(mol/Å) with the penalty functions in place. The lowest energy conformation obtained was minimized to a gradient of less than 0.01 kcal/(mol/Å) without any constraints in place. The resulting conformation was found to be consistent with the NMR-derived distance constraints.

Biological Data. Influenza virus N9 sialidase was incubated for 30 min at 37 °C in a buffer (MES, 6 mM $CaCl_2$, pH 6.5) containing either 30 mg/mL or 70 mg/mL fetuin and varying concentrations of inhibitor (antibody mimic (**5**) and linear peptide (**7**)). The sialic acid released by the enzyme was assayed according to the method developed by Warren[31] and then subsequently modified by Aminoff[32] and Aymard-Henry *et al.*[33]

Results and Discussion

Analysis. The determination of the components of recognition of the N9 sialidase–NC41 antibody complex involved a geometrical nonbonded analysis and an enthalpic calculation. The data from this analysis are summarized in Table 1. These data show, that in comparison to the antibody, CDR H3 (H96–H99) comprises 100% of the buried charge–charge contacts, 79% of the charge–polar contacts, 28% of the polar–polar contacts, 78% of the charge–nonpolar contacts, 16% of the nonpolar–nonpolar contacts, and 44% of the hydrogen bonds. Hydrogen bonds are considered as a separate class of polar contacts in this analysis procedure. The intermolecular energy of the interaction was calculated using the anal module of AMBER. This antibody loop comprised 52% of the total intermolecular energy of the entire antibody. Thus, enthalpically at least four amino acids seem to contribute a significant portion of the interaction energy of the complex.

It has been suggested that one of the greatest free energy deficits in protein complexation results from the requirement to desolvate hydrophilic functional groups.[34,35] This is a result of water participating in strong interactions with hydrogen-bond donors and acceptors as well as in neutralizing charged side chains. Due to the geometric constraints of protein molecules, the hydrophilic side chains buried in the protein complex would participate in fewer hydrogen bonds than they would in the undissociated form, when both donors and acceptors are fully water accessible. As a result, the desolvation of these hydrophilic groups, that do not hydrogen bond within the complex, is an expensive component of complexation. A crude estimation of this unfavorable component of complexation can be achieved by identifying the hydrogen-bond donors and acceptors on the protein-combining sites that are not hydrogen bonding within the complex but are hydrogen bonding with water in the undissociated state. This should give some indication of how many hydrogen bonds are lost on complex formation, in comparison to those made with water, and which residues are responsible for this loss.

The hydrogen-bonding capacity of the antibody recognition site in the undissociated state was characterized by solvating the antibody binding site with an 8.0-Å layer of water molecules. The lowest energy conformation found, from the molecular dynamics study, was used in the analysis procedure. It was found that loop CDR H3 only buries two atoms upon complexation that are hydrogen bonding to the solvent and not with the protein, in comparison to the entire antibody which buries 14 such atoms. This loop makes a total of 10 hydrogen bonds to the antigen, and therefore does not appreciably contribute to complex destability.

Some measure for the role of the electrostatic interactions in protein–protein complexation has been obtained by the above analysis procedure. However, it has been suggested by others that hydrogen bonds and electrostatic and van der Waals interactions contribute little to the stability of protein interactions.[34,35] This is because these interactions replace similar ones made with solvent molecules in the unbound species. Their main role is thought to confer specificity. One aspect of this study was

(29) *Felix 1.0 program*; Hare Research, Inc.: Woodinville, WA, 1990.
(30) Kuntz, I. D.; Thomason, J. F.; Oshiro, C. M. *Methods Enzymol.* **1989**, *177*, 199–205.
(31) Warren, L. *J. Biol. Chem.* **1959**, *234*, 1971–1975.
(32) Aminoff, D. *Biochem. J.* **1961**, *81*, 384–392.
(33) Aymard-Henry, M.; Coleman, M. T.; Dowdle, W. R.; Laver, W. G.; Schild, G. C.; *Bull. W. H. O.* **1973**, *48*, 199–202.
(34) Chothia, C. H.; Janin, J. *Nature* **1975**, *256*, 705–708.
(35) Janin, J.; Chothia, C. H. *J. Mol. Biol.* **1976**, *100*, 197–211.

to investigate the hydrophobic contributions[34-37] of complex formation. Whilst under a great deal of conjecture lately,[38] one view is that the hydrophobic effect can be considered as an absence of hydrogen bonding between nonpolar molecules and water, rather than a favorable interaction between the nonpolar groups themselves. The hydrophobic effect can be considered as an entropic force.[37] The favorable entropy term arises due to the release of water molecules upon complexation. This is consistent with the "cavity"[37,39] model, in which the first step may be regarded as the formation of a cavity in water into which the solute will fit. The free energy of formation of such a cavity in liquid water will be large because it requires the separation of strongly interacting water molecules. Once the cavity is formed and the solute placed in it, the solvent will undergo any further changes that reduce the free energy of the system. With a polar solute, hydrogen bonds and other electrostatic interactions will compensate for the initial energy required to form the cavity. However, a nonpolar solute will gain only the minor van der Waals forces with the solvent. To compensate for the absence of favorable electrostatic interactions with the solute, the solvent surrounding it will rearrange to form the most extensive number of hydrogen bonds between water molecules. The water molecules are therefore "immobilized" on the binding surface and significantly contribute to the hydrophobic effect when two nonpolar molecules interact.

The preceding analysis of the solvation of the binding surface of antibody NC41 permits a crude estimation of the hydrophobic effect. As an initial oversimplified estimate of hydrophobicity, an estimation of the number of "immobilized" water molecules on the protein binding surface was required. An "immobilized" water molecule is defined as a water molecule that does not hydrogen bond with the protein and interacts with the nonpolar atoms of the protein. It is these water molecules that are thought to contribute a significant portion of the hydrophobic effect.[40]

The previously calculated low-energy solvated conformation was analyzed by the program CONTACT in order to identify the "immobilized" water molecules on the protein binding surface. The antibody binding site comprises 63 such water molecules. Of these, 21 (one-third) are with the loop CDR H3. This simplistic estimation of hydrophobicity tends to suggest that loop CDR H3 contributes approximately one-third of the hydrophobic force of the entire protein. In addition, upon binding to the antigen this loop would displace approximately 17 immobilized waters on the antigenic surface. Upon complexation this loop buries a total of 204 Å^2 of surface area.[8] This is approximately one-third of the entire protein, and such information qualitatively suggests that this loop would contribute a significant amount[34,41,42] to the hydrophobic effect.

Collectively, from this analysis, it appears that one loop on antibody NC41 (CDR H3) contributes a significant portion of the interaction energy. In the complex, CDR H3 forms a ridge which matches a shallow depression on N9 lined by residues in the active site loop 367–372, loop 400–403, and loop 430–435. The side chain of Asn H98 of the antibody protrudes from the surface and interdigitates between the side chains of Thr 401 and Trp 403. A buried salt link exists between Lys 432 of sialidase N9 and Asp H97 of the antibody. The complex has been described in more detail elsewhere.[8]

(36) Kauzmann, W. *Adv. Protein Chem.* **1959**, *16*, 1–64.
(37) Creighton, T. E. *Proteins Structure and Molecular Properties*; WH Freeman and Co.: New York, 1984.
(38) (a) Privalov, P. L.; Gill, S. J. *Adv. Protein Chem.* **1988**, *39*, 191–234. (b) Privalov, P. L. *Annu. Rev. Biophys. Biophys. Chem.* **1989**, *18*, 47–69. (c) Privalov, P. L.; Gill, S. J. *Pure Appl. Chem.* **1989**, *61*, 1097–1104. (d) Murphy, K. P.; Privalov, P. L.; Gill, S. J. *Science* **1990**, *247*, 559–561. (e) Muller, N. *TIBS* **1992**, *17*, 459–463.
(39) Gill, S. J. *J. Phys. Chem.* **1985**, *89*, 3758–3761.
(40) Andrews, P.; Tintelnot, M. *Comprehensive Medicinal Chemistry*; **1990**, *4*, 321–348.
(41) Nemethy, G.; Scheraga, H. A. *J. Phys. Chem.* **1962**, *66*, 1773–1789.
(42) Forsythe, K. H.; Hopfinger, J. A. *Macromolecules* **1973**, *6*, 423–437.

Table 2. Summary of the Design Data (in kcal/mol)

conformation	energy	RMS[a]	E_{min}	induction energy
E_{con}	7.7	0.2	4.6	3.1
E_{force}	97	0.6	89	8

[a] Root mean square of the E_{con} conformation is with the five atoms defining the receptor framework. Root mean square of the E_{force} conformation is over all the side-chain atoms.

As mentioned above, the antibody loop (CDR H3) makes direct contact with the N9 active-site loop 368–370. The analysis data, taken together with the hypothesis that antibody NC41 inhibits N9 sialidase activity by binding to the active-site loop 368–370,[16] present the opportunity for the design and synthesis of a compound that mimics these antibody loop amino acids. This mimic may also bind to the active-site loop 368–370 and therefore sterically interfere with enzyme catalysis.

Design. In the preceding analysis section we have described a theoretical technique used to identify several amino acids out of the 20 or so which comprise the antibody recognition site that appear to be responsible for molecular recognition. On the basis of the receptor-bound conformation of these amino acids, known from the protein crystal structure, a design strategy toward suitable cyclic constraints that would hold the peptide sequence in the preferred receptor-bound conformation was required.

Conformational constraints can be separated into two classes.[43,44] The first group, "local" conformational constraints, is used to modify the local conformation to a specific or highly restricted conformation.[43] Their utilization is best undertaken within the context of a structure that already provides a measure of conformational stability, such as a β-turn or an α-helix. The second group, "global" constraints,[43,44] promotes or stabilizes more comprehensive structural features such as α-helices, β-sheets, β-turns, and loops, which are important or sometimes essential for the biological activity of the compound.[43]

Due to the precise steric and electronic requirements of the N9 sialidase–NC41 antibody recognition,[45] this stabilization should not interfere with the steric and electronic properties of this loop. The problem with the most commonly used global conformational constraints[43,44] is their inherent flexibility due to the inclusion of several rotatable sp^3 bonds. In order to circumvent this problem, it was decided to design rigid organic compounds ("scaffolds") that could bridge the C and N termini of the loop.

Design of Organic Scaffolds. In this study, the novel design approach involved the use of the receptor template geometry (defined in Figure 2) of the key loop as conformational constraints in the first phase of the design process. The atomic distances and dihedral angles defining the receptor framework of the key antibody loop (CDR H3) were calculated as 5.5 Å, 56.8°, and −55.6°, respectively (Figure 2). This data was used to identify rigid organic "scaffolds" that could energetically adopt the distance spanning the loop (C3–C4, Figure 2) and the C2–C3 and C4–N5 vectors (the receptor template). The results showed that 3-(aminomethyl)benzoic acid had a root mean square of 0.2 Å with the five atoms defining the receptor framework, and this conformation was only 3.1 kcal/mol above the lowest energy conformation found (Table 2, Figure 3). It was thus concluded 3-(aminomethyl)benzoic acid is a suitable rigid organic scaffold.

The ability of the constrained cyclic peptide to adopt the desired receptor conformation was tested using the template force technique.[46] In this technique the root mean square difference

(43) Hruby, V. J.; Al-Obedi, F.; Kazmieski, W. *Biochem. J.* **1990**, *268*, 249–262.
(44) Hruby, V. J. *Life Sci.* **1982**, *31*, 189–199.
(45) Webster, R. G.; Air, G. M.; Metzger, D. W.; Colman, P. M.; Varghese, J. N.; Baker, A. T.; Laver, W. G. *J. Virol.* **1987**, *61*, 2910–2916.
(46) Struthers, R. S.; Hagler, A. T In *Conformationally Directed Drug Design. Peptides and Nucleic Acids as Templates or Targets*; Vida, J. A., Gordon, M., Eds.; American Chemical *Society*: Washington, DC, 1984; pp 239–261.

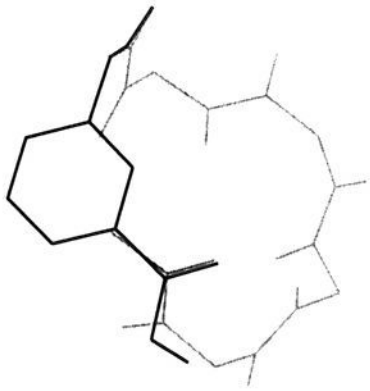

Figure 3. Illustration of superimposition of E_{cons} onto the desired receptor template.

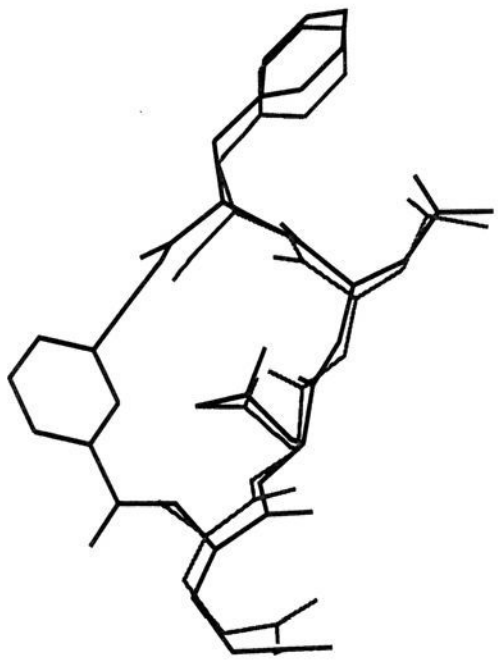

Figure 4. Superimposition of template force conformation (black) onto the desired receptor-bound conformation (gray).

between the analogue (constrained cycle peptide) and the template (desired loop conformation) is minimized simultaneously with the potential energy of the analogue. By minimizing this combined function, the lowest energy conformation (E_{force} conformer) is found that achieves a given fit of the analogue to the template. By conformational searching, and calculation of a low-energy conformer (E_{min} conformer), the energy required (induction energy) to achieve the desired receptor-bound conformation can be calculated. The data from these calculations is summarized in Table 2 and in Figure 4. The amount of energy required to induce the lowest found *in vacuo* conformation into the receptor-bound conformation was calculated as 8 kcal/mol.

Synthesis. The synthesis of the organic scaffold is shown in Figure 5. 3-(Phthalimidomethyl)benzoic acid (**1**) was prepared in 80% yield by the treatment of benzoic acid with *N*-(hydroxymethyl)phthalimide[25,47] in 90% sulfuric acid at 0 °C. The phthaloyl protecting group 3-(phthalimidomethyl)benzoic acid (**1**) was removed under mild conditions by reduction with sodium borohydride.[48] The final step required the protection of the amino functional group as its Fmoc derivative and was achieved by treatment of **3** with (9-fluorenylmethyl)succinimidyl carbonate at a pH of 8.

The syntheses of the precursor peptides for the cyclic lactam analogues of the antibody mimic (**5**) were accomplished by the solid-phase synthetic methods summarized in Figure 5. After neutralization of the pMBHA resin, the β-carboxyl group of the first amino acid (Asp) was coupled to the resin as its preformed HOBt ester. An *N*-capping procedure was then employed, to acylate any free amino groups on the resin. Importantly, it is the β-carboxyl of Asp that is attached to the pMBHA resin; this leaves an α-carboxyl suitably protected for cyclization. Cleavage

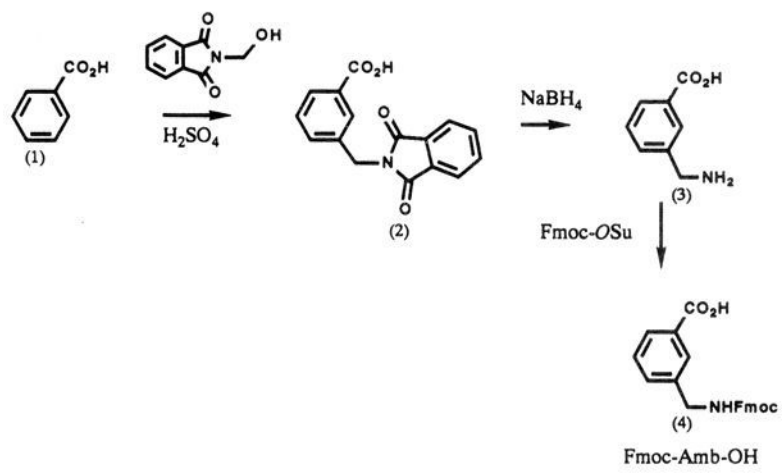

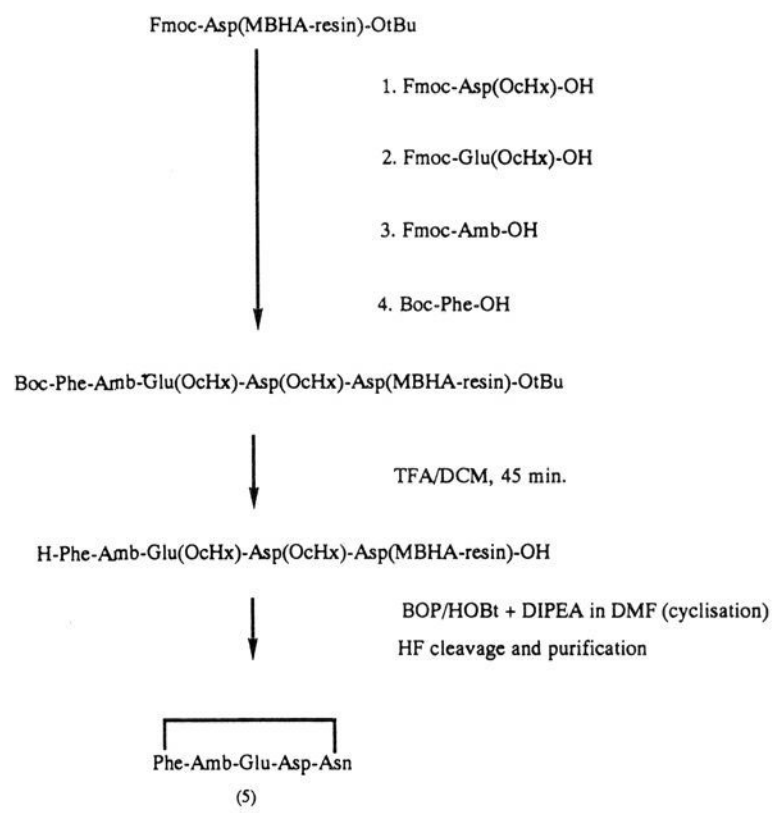

Figure 5. Synthesis of antibody mimic.

from the resin will result in the production of a β-amide and hence an Asn at this position. The remaining amino acids (Fmoc–Glu(OcHx)OH, Fmoc–Amb(OH), and Boc–Phe(OH)) were added using the BOP/HOBt procedure. Prior to cyclization whilst bound to the resin, deprotection of both the *N*-terminal Boc and *C*-terminal *t*Bu functional groups was achieved with 60% TFA/DCM. It was decided to cyclize whilst bound to the resin, as this is reported[26,49] to give products of a higher yield and purity.

Resin cyclization was initially attempted with DCC/HOBt; however, the major product isolated from this synthesis was the $O \rightarrow N$ acyl migration product.[18,50] Cyclization using BOP/HOBt was then attempted, and the desired constrained cyclic peptide (**5**) was isolated (Figure 6). The cyclization reaction required 5 days to go to completion and was monitored by the quantitative ninhydrin assay. The imide byproduct (**6**) was also detected (Figure 6) and was characterized by the lack of DQFCOSY crosspeak between Asn Cα to the NH region and the ROESY crosspeak from the NH of Asp to the Cα of Glu. Imide formation during cyclization reactions has been previously documented;[26] though it is reported to be significantly reduced by the use of cHx-protected amino acids. The unconstrained peptide (**7**) was synthesized using standard Boc solid-phase peptide synthesis methodologies.

(47) (a) Zaugg, H. E. *Synthesis* **1970**, 49–73. (b) Zaugg, H. E. *Synthesis* **1984**, 85–110.

(48) Osby, J.; Martin, M. G.; Ganem, B. *Tetrahedron Lett.* **1984**, *25*, 2093–2096.

(49) (a) Felix, A. M.; Wang, C. T.; Heimer, E. P.; Fournier, A. *Int. J. Pept. Protein Res.* **1988**, *31*, 231–238. (b) Felix, A. M.; Heimer, E. P.; Wang, C.; Lambros, T. J.; Forunier, A.; Mowles, T. F.; Maines, S.; Campbell, R. M.; Wegrzynski, B. B.; Toome, V.; Fry, D.; Madison, V. S. *Int. J. Pept. Protein Res.* **1988**, *32*, 441–454. (c) Schiller, P. W.; Nguyen, T. M.; Miller, J. *Int. J. Pept. Protein Res.* **1985**, *25*, 171–177.

(50) Burke, T. R.; Knight, M.; Chandrasekhar, B. *Tetrahedron Lett.* **1989**, *30*, 519–522.

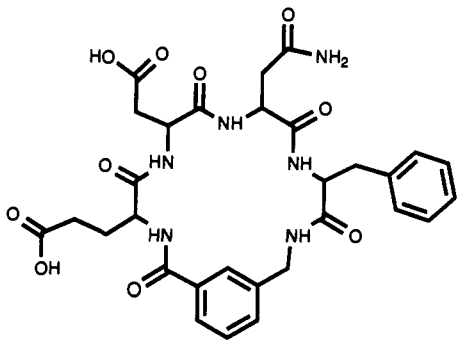

(5)

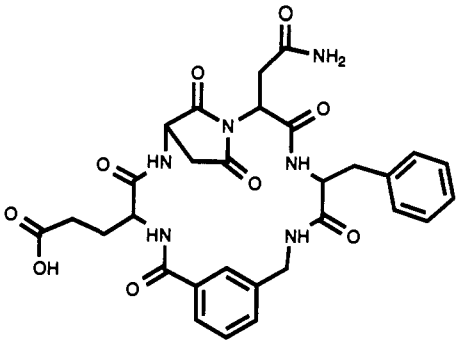

(6)

Figure 6. Structures of the biologically active antibody mimic **5** and the observed imide byproduct **6**.

Table 3. Chemical Shifts[a] and $^3J_{NH-H\alpha}$ Coupling Constants[b] of Antibody Mimic (**5**) in d_6-DMSO at 30 °C

	chemical shift (ppm)			
residue	NH	CαH	CβH	other
Glu	8.60 (6.0 Hz)	4.20	1.97	CγH$_2$, 2.40
Asp	8.44 (11.5 Hz)	4.53	2.64, 2.95	
Asn	7.86 (8.3 Hz)	4.33	2.64	
Phe	8.31 (7.6 Hz)	4.48	2.67, 3.12	C2,3,4,5,6H, 7.18–7.42
Amb	8.48 (5.8 Hz)			CH$_2'$, 4.20, CH$_2''$, 4.49, C2H, 7.80, C6H, 7.66, C4H, C5H, 7.42.

[a] Chemical shifts are referenced to the d_6-DMSO peak at 2.49 ppm. [b] Coupling constants were measured from the DQFCOSY spectrum.

Table 4. Temperature Dependence[a] of NH Peaks of Antibody Mimic (**5**) in d_6-DMSO

temp (K)	Glu NH	Amb NH	Asp NH	Phe NH	Asn NH
298	8.544	8.425	8.344	8.230	7.762
303	8.514	8.400	8.336	8.225	7.755
310	8.482	8.373	8.327	8.216	7.745
315	8.450	8.341	8.312	8.206	7.735
coeff (ppm/K)	-6.3×10^{-3}	-5.6×10^{-3}	-2.1×10^{-3}	-1.6×10^{-3}	-1.8×10^{-3}

[a] Chemical shifts (ppm) are referenced to an aromatic peak at 7.42 ppm.

NMR. The ^{1}H spectra of the target molecule (**5**), byproduct (**6**), and linear peptide (**7**) were assigned by a combination of DQFCOSY and ROESY experiments. The assignments of the antibody mimic are summarized in Table 3. The temperature dependencies of the amide protons of the antibody mimic (**5**) were measured in d_6-DMSO and are shown in Table 4. These data indicate that the Asp, Asn, and Phe backbone NH's are strongly hydrogen-bonded, whilst the constraint (Amb) and Glu NH's are in conformational equilibrium between stable hydrogen-bonded conformations and the solvent-exposed environment.[51]

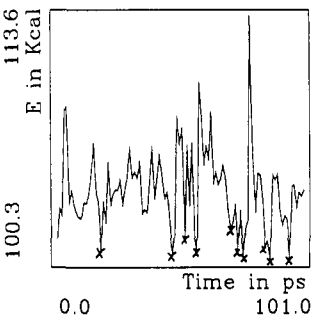

Figure 7. Energy of the 100 minimized structures sampled during the 100-ps (800 K) molecular dynamics search. The low-energy conformations superimposed in Figure 8 are indicated by X's.

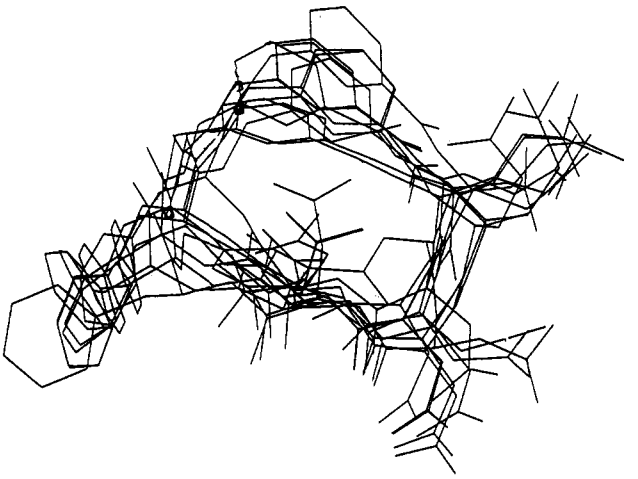

Figure 8. Superimposition of the 10 lowest solution conformations found over a 100-ps molecular dynamics simulation.

The solution conformation of the antibody mimic (**5**) was calculated by a combination of restrained molecular dynamics and restrained molecular mechanics. In total, 100 conformations were collected during the restrained molecular dynamics conformational search. Each of these 100 structures was superimposed onto the side-chain atoms of the desired receptor loop conformation. The root mean square of these 100 conformations, with the desired receptor-bound conformation, had a value between 3.0 and 4.0 Å. A plot of the energy of the 100 structures versus time is presented in Figure 7. The 10 low-energy conformations shown in Figure 7 were obtained for further analysis. The superimposition of these 10 structures is illustrated in Figure 8. The lowest energy conformation found was minimized without the constraints in place. It had an energy of 90 kcal/mol and was found to be consistent with the distance constraints derived from NMR. The energy of the desired receptor-bound conformation was calculated at 95 kcal/mol in the design process. Therefore it would appear as though the organic "scaffold" has stabilized the cyclic peptide to conformations that are energetically close to the desired receptor-bound conformation.

Biological Data. CDR H3 has been shown (theoretically) to be essential for recognition between the antibody and the antigen. Since CDR H3 binds directly to active-site loop (368–370) on the antigen, the antibody mimic may also bind to this region. If this does occur, then it is possible that the antibody mimic can sterically interfere with the approach of the large substrate fetuin and inhibit enzyme activity.

In fact, a K_i of 1×10^{-4} M was determined for the antibody mimic (**5**) using the naturally occurring substrate fetuin against N9 sialidase. These data are shown as Dixon plots in Figure 9.

(51) (a) Hruby, V. J. *Chem. Biochem. Amino Acids, Pept., Proteins* **1974**, *3*, 1–188. (b) Kemp, D. S.; McNamara, P. *Tetrahedron Lett.* **1982**, *23*, 3761–3769.

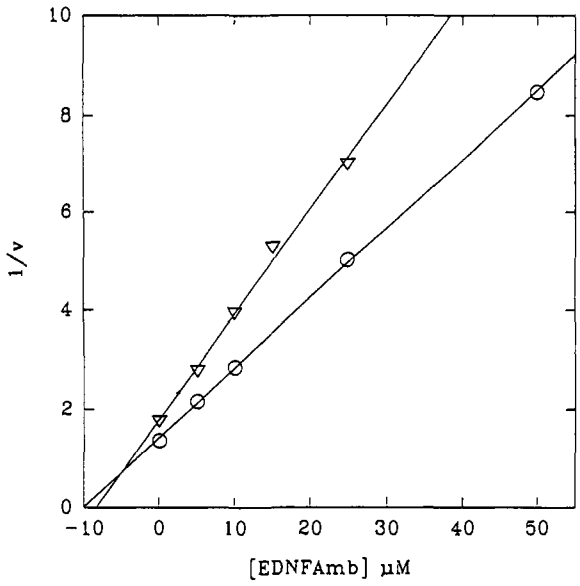

Figure 9. Dixon plot for the inhibition of influenza virus N9 sialidase by the antibody mimic **5** with fetuin as the substrate: ▽, 30 mg/mL fetuin; ○, 70 mg/mL fetuin. $1/v$ is in fluorescence units.

These data clearly indicate that the antibody mimic (**5**) is an inhibitor of the influenza viral enzyme, N9 sialidase. Inhibition produced by the antibody has been previously noted.[7,8,14,15] Since the antibody mimic was designed to bind at the same epitope region as the antibody NC41, it is reasonable to suggest that an inhibition similar to the inhibition observed with NC41 occurs. Indeed the current data supports the notion that the antibody mimic acts in a similar fashion to the antibody NC41. The linear peptide (**7**) did not inhibit enzyme activity, illustrating the importance of the constraint in achieving molecular recognition and hence inhibition of the enzyme.

An alternative explanation to the current interpretation might be that the mimic is binding directly in the active site. However, this is considered unlikely because of the size of the mimic. A study of the dimensions of the active site appears to preclude the mimic from both entering and binding at this site. The antibody mimic was designed to bind at the edge of the active site on loop 368–370 and may inhibit the enzyme by binding to this loop. This is supported by the fact that the mechanism of antibody NC41 inhibiting N9 sialidase is thought to be due to the antibody binding to this same loop.[16]

The mimetic binds approximately 3 orders of magnitude less than that of the parent protein. The antibody mimic contains only four out of the 17 or so residues of the antibody that form contacts with the antigen N9 sialidase. As well, considering the large difference in bound surface area between the antibody–antigen complex and the antibody mimetic–antigen complex, one would imagine that the mimetic would bind with a lower affinity than the parent protein. However, it is possible to improve the affinity of the mimetic by further restricting its available conformational space. The inclusion of local constraints[43,44] may further restrict the conformation of the mimetic to regions about the desired receptor-bound conformation. This would effectively deplete alternative conformations that don't bind and therefore increase binding affinity. This is consistent with the strategy of using global conformational constraints (such as 3-(aminomethyl)-benzoic acid) to stabilize the structural features of the loop, followed by local conformational constraints to further restrict backbone conformations to regions around the desired receptor-bound conformation.

Conclusion

We have analyzed the antibody NC41-N9 sialidase crystal structure and identified one loop on the antibody (CDR H3) that appears to theoretically contribute a significant proportion of the interaction energy between the complex. A constrained cyclic peptide was theoretically designed to mimic the receptor-bound conformation of these key amino acids. The designed organic constraint was synthesized followed by the preparation of the constrained cyclic peptide (antibody mimic) using standard solid-phase synthesis protocols. The desired receptor-bound conformation of the antibody mimic was only 5 kcal/mol higher than the solution (d_6-DMSO) conformation. The biological activity of this low molecular weight compound suggests that it is mimicking the binding function of antibody NC41.

Acknowledgment. We would especially like to thank Prof. P. R. Andrews for his help in the initial stages of the project and the reading of this manuscript. We would also like to thank Dr. P. Colman, Dr. W. Tulip, and Dr. J. Varghese and colleagues for the coordinates of the sialidase N9 antibody NC41 complex and many helpful discussions. We would also like to thank Dr. M. Pegg and Ms. F. Rose for technical assistance in biological testing, Mr. Jeff Dyason for assistance in the preparation of this manuscript, and K. Nielsen for technical assistance in NMR. We would like to thank the National Health and Medical Research Council for financial support, and (M.L.S.) would like to thank Biota Holdings Ltd for a postgraduate fellowship.